

# Role of non-linear data processing on speech recognition task in the framework of reservoir computing

Flavio Abreu Araujo<sup>1,\*</sup>, Mathieu Riou<sup>2</sup>, Jacob Torrejon<sup>3</sup>, Sumito Tsunegi<sup>4</sup>, Damien Querlioz<sup>5</sup>, Kay Yakushiji<sup>4</sup>, Akio Fukushima<sup>4</sup>, Hitoshi Kubota<sup>4</sup>, Shinji Yuasa<sup>4</sup>, Mark D. Stiles<sup>6</sup>, and Julie Grollier<sup>2</sup>

<sup>1</sup>Institute of Condensed Matter and Nanosciences, Université catholique de Louvain, Place Croix du Sud 1, 1348 Louvain-la-Neuve, Belgium

<sup>2</sup>Unité Mixte de Physique, CNRS, Thales, Université Paris-Sud, Université Paris-Saclay, 91767 Palaiseau, France.

<sup>3</sup>Service de Physique de l'Etat Condensé, DSM/IRAMIS/SPEC CNRS UMR 3680 CEA Saclay, 91191 Gif-sur-Yvette Cedex, France

<sup>4</sup>National Institute of Advanced Industrial Science and Technology (AIST), Spintronics Research Center, Tsukuba, Ibaraki 305-8568, Japan.

<sup>5</sup>Centre de Nanosciences et de Nanotechnologies, CNRS, Université Paris-Sud, Université Paris-Saclay, 91405 Orsay, France

<sup>6</sup>Center for Nanoscale Science and Technology, National Institute of Standards and Technology, Gaithersburg, Maryland 20899-6202, USA.

\*flavio.abreuaraujo@uclouvain.be

## ABSTRACT

The reservoir computing neural network architecture is widely used to test hardware systems for neuromorphic computing. One of the preferred tasks for bench-marking such devices is automatic speech recognition. However, this task requires acoustic transformations from sound waveforms with varying amplitudes to frequency domain maps that can be seen as feature extraction techniques. Depending on the conversion method, these may obscure the contribution of the neuromorphic hardware to the overall speech recognition performance. Here, we quantify and separate the contributions of the acoustic transformations and the neuromorphic hardware to the speech recognition success rate. We show that the non-linearity in the acoustic transformation plays a critical role in feature extraction. We compute the gain in word success rate provided by a reservoir computing device compared to the acoustic transformation only, and show that it is an appropriate bench-mark for comparing different hardware. Finally, we experimentally and numerically quantify the impact of the different acoustic transformations for neuromorphic hardware based on magnetic nano-oscillators.

## Introduction

Artificial neural network algorithms outperform humans on recognition tasks like image or speech recognition, by leveraging deep networks of interconnected non-linear units called formal neurons<sup>1</sup>. The goal of neural networks is to extract the features and classify input data through learned non-linear transformation. Running such algorithms on a classical computer is costly energetically: to overcome this issue, neuromorphic approaches<sup>2,3</sup> propose to implement them physically. In particular, reservoir computing<sup>4,5</sup> is a kind of recurrent neural network that has been widely used to test the efficiency of hardware for neuromorphic computing<sup>6-8</sup> because it has a simplified architecture and learning procedure. The input is sent to a neural network with fixed recurrent connections called a reservoir. The goal of the reservoir is to separate the different kinds of inputs, such that after this transformation, the classification can be done by a linear transformation. The response of the neurons of the reservoir are combined linearly with trained connections to construct the output. Since the connections in the reservoir are random and fixed, it is easier to fabricate it in hardware and then train the output connections, often emulated in software, with linear regression.

Speech recognition is a widely used class of benchmark tasks performed to test the efficiency of a neural network. It is especially employed in the case of reservoir computing because the recurrent connections of the reservoir create an intrinsic memory that is useful to classify time-varying inputs. Generally, this task requires frequency decomposition<sup>9-11</sup> prior to the neural network because the acoustic features are contained in the frequency rather than in the amplitude of the time-varying

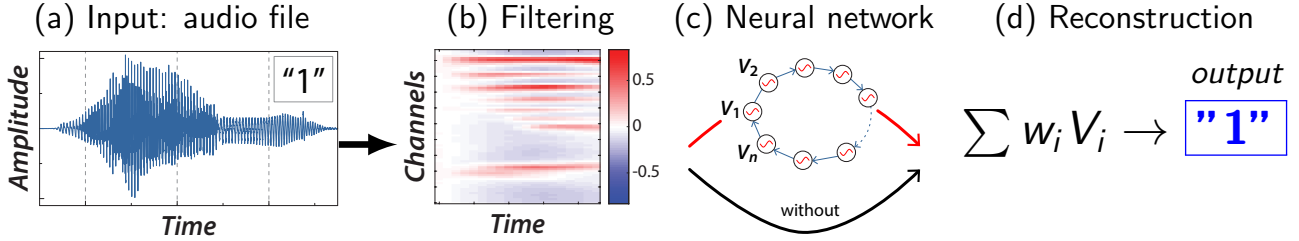


**Figure 1. Principle of spoken digit recognition.** (a) Audio waveform corresponding to the digit 1 pronounced by speaker 1. (b) Filtering to frequency channels for acoustic feature extraction. The signal during each time interval  $\tau$  is decomposed in  $N_f$  frequency channels. The cochlear model filters each point of the audio waveform in 78 frequency channels (13 in the case of the MFCC model and 65 for the spectrogram model). The frequency channels are concatenated in intervals of duration  $\tau$  to form the filtered input. (c) The filtered input is injected in the neural network or directly used to construct the output (No neural network). The neural network is composed of  $N$  interconnected filtered inputs. (d) For each digit, the response of the neural network (or directly the filtered output) is constructed from a linear combination of neuron states  $V_i$  (there are 10 classifiers in total).

signal. These decompositions return the amplitude of the signal in different frequency channels as a function of time. The neural network then extracts the acoustic features contained in the frequency information. Several frequency decomposition methods have been reported in the literature: Mel-frequency cepstral coefficients (MFCC) and Lyon's cochlear model (cochleagram) are the most common methods since they mimic the filtering that occurs biologically<sup>9, 12, 13</sup>. However, the actual contribution of the acoustic filter to the total speech recognition rate is generally not investigated while performing speech recognition benchmarks with reservoir computing hardware, possibly implying that its influence on the final recognition rate is negligible<sup>8</sup>. Furthermore, both of these methods were developed before machine learning became popular and, thus they were designed to extract the useful features of an audio signal independent of modern machine learning.

Here, we show how the choice of different filtering methods drastically affects the final speech recognition rate. We quantify the contributions of the acoustic filtering and the neural network, respectively, for a spoken digit recognition task using three frequency decomposition methods with different non-linear characters: non-linear cochleagram, MFCC, and linear spectrogram. In a first step, we show that the cochleagram and the MFCC filter are powerful stand-alone features extractors and that they can achieve for themselves (without any additional machine learning technique) very high recognition levels: up to 95.8 % and 77.2 % for cochleagram and MFCC, respectively. In contrast, the linear spectrogram never achieved recognition levels statistically better than random sampling, 10 %. However, by adding various levels of non-linearity to the real part of the spectrogram we were able to show a large increase of the recognition rate from about 10 % (linear) to 88 % (strong non-linearity). These results indicate that the high recognition level of the cochleagram and MFCC approaches is mainly due to the non-linear character of these frequency decomposition methods.

In a second step, we evaluate the gain in recognition rate provided by a particular hardware approach to reservoir computing, based on magnetic nano-oscillators. In order to compare to other hardware implementations in the literature, we model a neural network based on a single dynamical non-linear magnetic node in the framework of the reservoir computing approach<sup>6-8, 14-16</sup>. We find that the contribution of the neural network is dominant for linear spectrogram filter and only plays a small role for the non-linear cochleagram and MFCC filter. Finally, we present experimental results using a non-linear and tunable magnetic nano-oscillator exhibiting an excellent agreement with our simulations.

## Methods

We perform a benchmark task called spoken digit recognition that is common in the reservoir computing community for software<sup>10</sup> and hardware<sup>7, 8, 14, 17-19</sup> implementations. The input data, taken from the TI-46 database, are audio waveforms of isolated spoken digits (0 to 9) pronounced by five different female speakers, Fig. 1a. Each speaker pronounces each digit 10 times. Each of these times is referred as "utterance". The goal is to recognise the digits, independently of the speaker and of the utterance. For that purpose, three different filtering methods were used: cochleagram, MFCC filter and spectrogram (the most common filtering method in the reservoir computing community is the cochleagram). The filters break the word in several time intervals  $N_\tau$  of duration  $\tau$  and analyse the frequency content in each interval  $\tau$  either through Fourier transform (spectrogram, 65 channels,  $N_\tau$  = 24 to 67 depending on the digit) or a more complicated non-linear approach (cochleagram, 78 channels,  $N_\tau$  = 16 to 41 and MFCC 13 channels,  $N_\tau$  = 31 to 83 depending on the digit). After the filtering, the input for each word is composed of an amplitude for each of  $N_f$  frequency channels times  $N_\tau$  time intervals, Fig. 1b.

The contribution of the frequency filtering and the reservoir computing, respectively, are then analysed separately. In order to evaluate the impact of the frequency filtering on the input separation capability, a linear classifier is trained directly on the different frequency channels. The classification results with both influence of the frequency filtering and the reservoir are computed by injecting the filtered input in a neural network composed of  $N_\theta$  interconnected neurons. Here, we use  $N_\theta = 400$  input neurons that are connected to all of the frequency channels for each time interval  $\tau$ , Fig. 1c. In the framework of reservoir computing, these fixed connections have random weights. To reach high classification rate, 400 neurons are sufficient<sup>6,8</sup>. The features of the magnetic neurons that we consider are specified in section IV. A linear classifier is trained to map the neuron outputs to the desired results. The contribution of the reservoir to the ultimate success is extracted from the results by subtracting the success rate found using only the frequency filtering methods.

In practice, the output signal is constructed from the linear combination (linear classifier) of the states  $V_i$  of each neuron (or each frequency channel  $f_j$ ) for each digit according to  $V_{\text{out}} = \sum w_i V_i$  ( $V_{\text{out}} = \sum w_j f_j$  only for the filter case), Fig. 1(d). This post-processing consists of two distinct steps. The first is called the training (or learning) process and the second is called the classification (or recognition) process. The goal of training is to determine an optimal set of weights  $w_i$  ( $w_j$ ) for each desired digit. These weights are used to multiply the neurons states  $V_i$  (each frequency channel  $f_j$ ), which are then averaged over the  $N_\tau$  time intervals to give an output value,  $V_{\text{out}}$ , which should ideally be equal to the target value  $\tilde{V}_{\text{out}}$ : 1 for the correct digit and 0 for the rest. In the training process, a fraction of the utterances are used to train these weights and in the classification process, the rest of the utterances are used to test the performance of the recognition. The optimum weights are found by minimising the quadratic error between  $\tilde{V}_{\text{out}}$  and  $V_{\text{out}}$  for all the words used in the training. See more in details in ref.<sup>8</sup>.

## Acoustic filter: role of non-linearity

First, we compute the digit recognition rate as a function of the number of utterances used in training for the cochleagram and the MFCC methods as shown in Fig. 2(a). The recognition rate increases with the number of trained utterances and then saturates in the case of the cochlear model. It remains almost constant for the MFCC model. Both filters achieve a high recognition rate. In particular, the cochlear model is an excellent acoustic feature extractor with recognition rates up to 95.8 % (for 9 trained utterances) whereas the MFCC filter is less powerful, reaching recognition rates up to 77.2 %.

These filters are commonly used for speech recognition tasks, because of their similarity to audio signal processing in biological ears, which perform complex frequency decompositions with high non-linearities. Both MFCC and cochlear methods use non-linearities to transform the audio data. For MFCC the transformed representation corresponds to the log-energy of the Mel frequency filter output<sup>9</sup>. In the cochleagram approach, the main non-linear ingredient corresponds to a set of interconnected automatic gain controls<sup>12,13</sup>. The successful separation of the data achieved by these filtering methods appears to be due mainly to the non-linear character of the transformation with a moderate influence of the kind of non-linearity (similarly to reservoirs that can have different kinds of non-linearity that work).

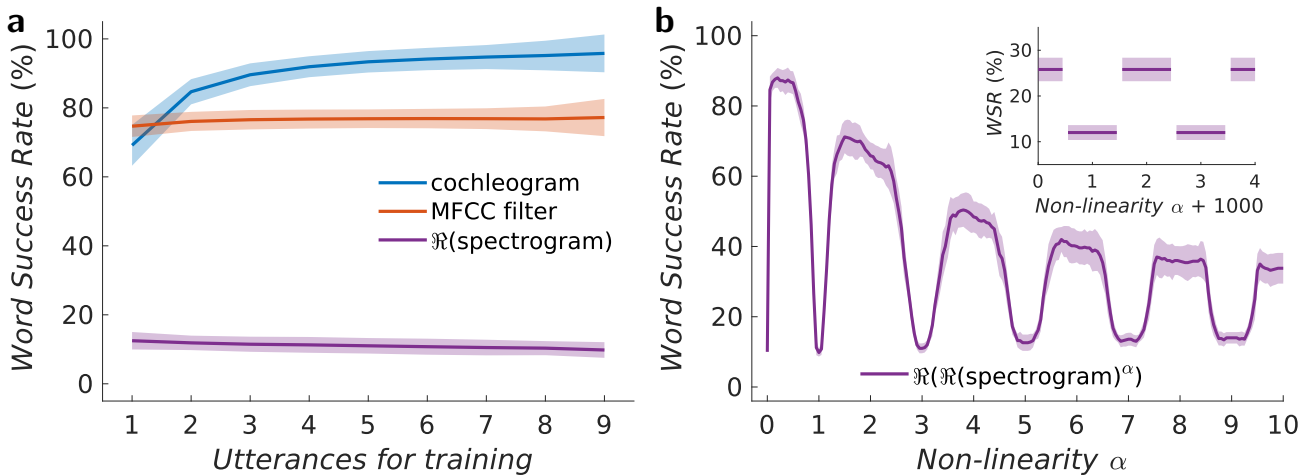


**Figure 2. Spoken digit recognition for filtered inputs.** (a) Spoken digit recognition rates as a function of the number of utterances  $N$  used for training of the filtered input (without neural network) corresponding to three different methods: cochleagram, MFCC filter and linear spectrogram ( $\alpha = 1$ ). (b) Spoken digit recognition as a function of non-linear coefficient for spectrogram methods (Inset: Word success rate for large non-linear coefficient values from 1000 to 1004). The coloured region corresponds to the uncertainty of the recognition rate, here the standard deviation).

To establish the critical role of the non-linearity contained in the filtering methods to recognition performance, we start by investigating the separation achieved by a very simple linear spectrogram filter. This filter is based on standard Fourier transforms of the audio input over finite time windows. The Fourier transform is a linear operation that outputs a real and an imaginary part. We consider only the real part in the following in order to avoid introducing non-linearities by computing the norm. After the Fourier transforms,  $Z_\sigma$  is the matrix of the real parts of the spectrogram with dimension  $N_f \times N_\tau$  where  $N_f$  is the number of frequency channels and  $N_\tau$  is the number of time steps, which depends on the particular digit. We normalise the data,  $X_\sigma = Z_\sigma / \max(|Z_\sigma|)$  and  $X_{ij,\sigma} \in [-1, 1]$  for  $i \in \{1..N_f\}$  and  $j \in \{1..N_\tau\}$ . The normalisation is crucial to ensure that there exists at least one  $X_{ij,\sigma}$  that is equal either to 1 or to -1 for each  $X_\sigma$  when non-linearities are introduced into the transform.

To study the influence of a non-linear transformation on the normalised input data  $X_\sigma$ , we choose to apply a point-wise operation, namely the exponent  $\alpha \in \mathbb{R}$ , giving rise to the transformation  $X_\sigma \rightarrow (X_\sigma)^\alpha$ . The impact of non-linear exponent  $\alpha$  on recognition rate is shown in Figure 2(b). The recognition rate strongly oscillates as a function of the non-linear exponent and decreases for large  $\alpha$ . Some particular values of the recognition rate can be easily understood. For  $\alpha = 0$ :  $\forall i$  and  $j$ ,  $X_{ij,\sigma} = 1$ , and it becomes impossible to discriminate between different digits  $X_\sigma$  and the success rate is equal to 10 % (random choice). As  $\alpha$  approaches zero, the success rate decreases drastically and drops to 10 %. For such exponents, all inputs get mapped to the same output making data separation impossible. For  $\alpha = 1$  the real part of the spectrogram corresponds to a linear transformation of the input data, thus there is no non-linear data separation and the word recognition rate  $\simeq 10$  % (random choice).

A finer understanding of the evolution shown in Figure 2(b) can be obtained by decomposing the exponent  $\alpha$  in an integer part  $n \in \mathbb{N}$  and a real part  $\varepsilon \in \mathbb{R}$  around  $n$  ( $\varepsilon \in [-0.5, 0.5]$ ):  $\alpha = n + \varepsilon$ . For  $X_{ij,\sigma} < 0$ ,  $X_{ij,\sigma}^- \rightarrow (X_{ij,\sigma}^-)^{n+\varepsilon} = |X_{ij,\sigma}^-|^{n+\varepsilon}(-1)^n(\cos(\pi\varepsilon) + i\sin(\pi\varepsilon))$  and for  $X_{ij,\sigma} \geq 0$ ,  $X_{ij,\sigma}^+ \rightarrow (X_{ij,\sigma}^+)^{n+\varepsilon} = |X_{ij,\sigma}^+|^{n+\varepsilon}$ . For simplicity, we choose to consider only the real part of the data obtained after applying the non-linearity, so  $R_\sigma = X_{ij,\sigma} \rightarrow \Re(X_{ij,\sigma}^{n+\varepsilon})$ :

$$R_\sigma = \begin{cases} \Re((X_{ij,\sigma}^-)^{n+\varepsilon}) = |X_{ij,\sigma}^-|^{n+\varepsilon}(-1)^n \cos(\pi\varepsilon) \\ \Re((X_{ij,\sigma}^+)^{n+\varepsilon}) = |X_{ij,\sigma}^+|^{n+\varepsilon} \end{cases} \quad (1)$$

From Eq. (1) and for  $X_{ij,\sigma} < 0$  there is an additional factor  $(-1)^n \cos(\pi\varepsilon)$ . Let's consider the particular case where  $\varepsilon = 0$ , then in the case of values of  $X_{ij,\sigma}$  that were initially negative, the values  $R_{ij,\sigma}$  that were equal to 1 for very large  $n$ , are multiplied by  $(-1)^n$ . So, depending on the parity of  $n$ , there are two different possibilities. If  $n$  is odd, there is at least one value  $R_{ij,\sigma}$  in  $R_\sigma$  equal to 1 for each  $R_\sigma$  (digit in the database). If  $n$  is even, the  $R_\sigma$  digits originating from an input  $X_\sigma$  where at least one  $X_{ij,\sigma} = -1$  have a corresponding  $R_{ij,\sigma} = -1$  (at least one  $R_{ij,\sigma} = 1$  otherwise). Therefore, the oscillating behaviour of the success rate shown in Fig. 2b can be entirely understood in terms of what happens to the negative input data as shown in Eq. (1) and the factor applied to negative values.

From Eq. (1) we can also evaluate the effect of our non-linear transformation for  $n \rightarrow \infty$ :  $\lim_{n \rightarrow \infty} |X_{ij,\sigma}|^n = 0$  for  $|X_{ij,\sigma}| < 1$  and  $\forall n |X_{ij,\sigma}|^n = 1$  when  $|X_{ij,\sigma}| = 1$ . In practice, due to the numerical truncation on a computer, for  $n \gg 100$  and  $|X_{ij,\sigma}| < 1$ ,  $|X_{ij,\sigma}|^n = 0$ . So, for very large  $n$ , the resulting vector  $R_\sigma$  contains only zeros and at least one element that is equal to 1 after the non-linear transformation.

There are 500 digits in our spoken digit database and for very large odd values of  $n$ , there are 253  $R_\sigma$  vectors with one  $R_{ij,\sigma} = 1$  and 247 with one  $R_{ij,\sigma} = -1$ . For large even values of  $n$ , all the 500  $R_\sigma$  contain one  $R_{ij,\sigma} = 1$ . So, for large values of  $n$ , there are 2 different success rate values depending on the parity of  $n$ . As shown in the inset of Fig. 2b, for large values of  $\alpha$  ( $\alpha > 1000$ ), the success rate behaviour tends to a square function alternating between very low values (12 %) around odd values of  $\alpha$ , i.e.  $\alpha \in [2n + 0.5, 2n + 1.5]$ , and a slightly higher value (25.8 %) around even values of  $\alpha$ , i.e. for  $\alpha \in [2n - 0.5, 2n + 0.5]$ , where  $n \in \mathbb{N}$  (for large values of  $\alpha$ , when  $\alpha = n + 0.5$ , the success rate is not defined).

Overall, as shown in Figure 2(b), for a wide range of values of  $\alpha$ , the non-linearity drastically improves the recognition rate. In particular, the recognition rate is very high for low exponents  $\alpha$ . An optimum non-linearity is reached for  $\alpha = 0.2$  providing the highest recognition rate of 88 %, which is comparable to those obtained for the cochleagram.

We use a  $t$ -Distributed Stochastic Neighbour Embedding ( $t$ -SNE) technique<sup>20</sup> to represent our  $N_f$  channels data in a 2D plot (see Fig. 3) in order to visualise how the data separation occurs and understand the recognition capacity of the different filtering methods.  $t$ -SNE is a nonlinear dimensionality reduction technique used for embedding high-dimensional data into a low-dimensional space of two or three dimensions. During the data reduction, the probability of two vectors to be neighbours is conserved, allowing visualisation of the structure in the data. Each digit is represented by coloured dots for all data points of the utterances. For instance, Fig. 3a shows that for the spectrogram with  $\alpha = 1$  (linear) for which the recognition rate is about 10 % (random choice), there is no data separation as all the coloured points seem to be randomly distributed. In particular the digits of a same class do not form separated clusters. On the other hand, for the spectrogram with  $\alpha = 0.2$  (optimal non-linearity), data separation can clearly be seen in Fig. 3b correlating with the better recognition rate of 88 % compared to the linear spectrogram

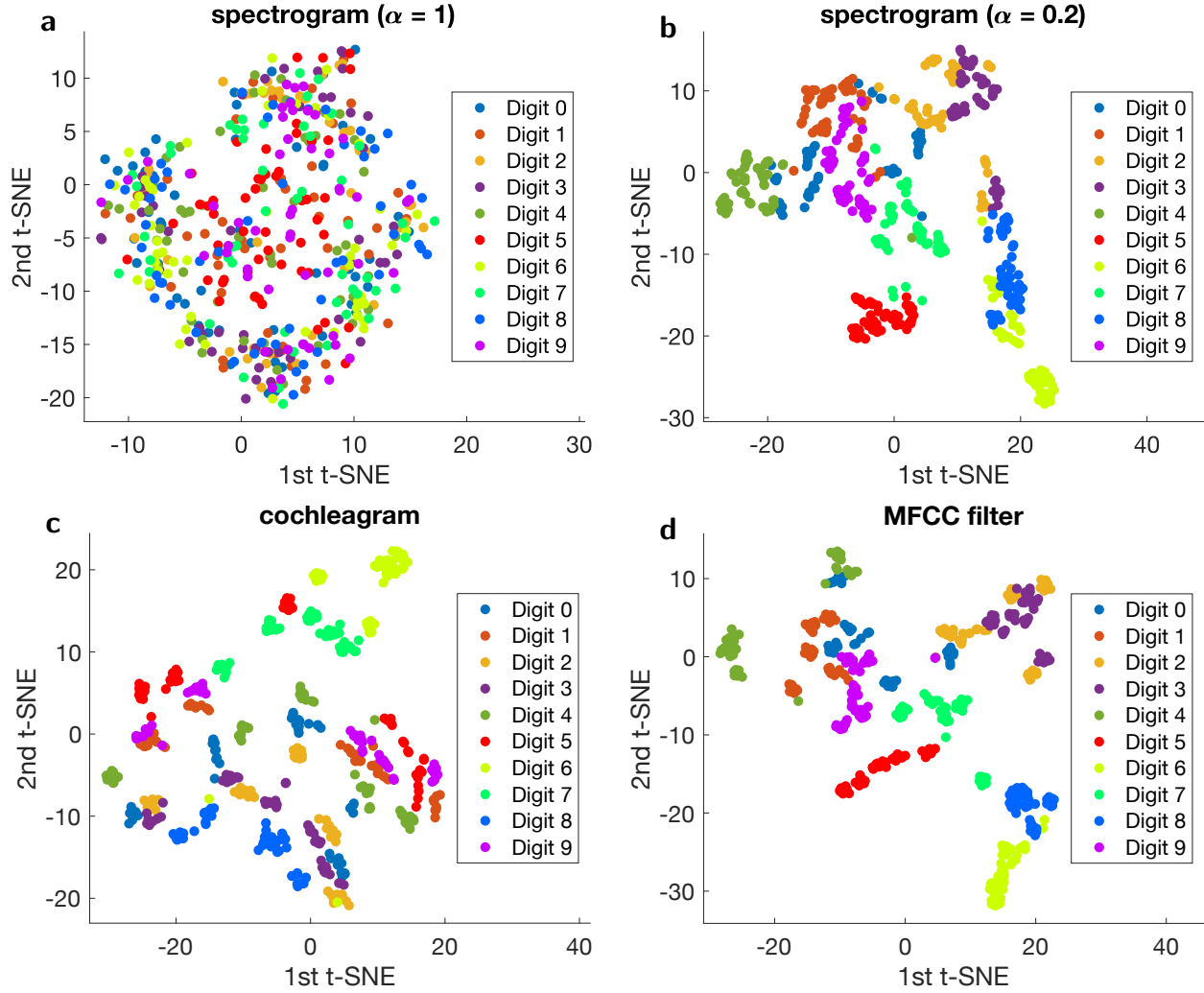


**Figure 3.** 2D representation of the two  $t$ -SNE components for: **a**, the spectrogram with  $\alpha = 1$ , **b**, the spectrogram with  $\alpha = 0.2$ , **c**, the cochleagram, and **d**, the MFCC filtering methods.

( $\alpha = 1$ ). Furthermore,  $t$ -SNE shows data separation capability for both the cochleagram and the MFCC filter. As shown in Fig. 3c and 3d, well defined clusters corresponding to the spoken digits appear and correlate well with the high recognition rates exhibited by the two filtering methods.

To summarise this section, we find that the MFCC filter and the cochleagram can play a similar role as the reservoir neural network in addition to filtering. We highlight that these stand-alone feature extractors perform data separation due to their internal non-linear transformations. We indeed obtain recognition performance that are close to what is found with these approaches by adding a simple non-linear transformation to the individual elements of the conventional spectrogram. Depending on the non-linearity exponent, the recognition rate can strongly vary from 10 % to 95.8 %.

## Neural network: Reservoir computing based on non-linear oscillators

Having shown that non-linear filtering methods can by themselves achieve high recognition rates, we turn to evaluating the gain in overall performance provided by a reservoir neural network taking as inputs the output of these acoustic filters. We implement the reservoir with a single non-linear oscillator<sup>6</sup>. In this approach, recurrent chains of non-linear transformations occur in time instead of space. The loss of parallelism is compensated by time-multiplexing, in turn requiring that the input be preprocessed. To do that, each point of interval  $\tau$  in Fig. 1(b) is multiplied by a random binary matrix (of dimensions  $N_f \times N_\theta$ ) to induce transient behaviour. This transformation is linear and does not affect the final recognition rate. Each point of the input audio file is converted in a binary sequence of duration  $\tau$  composed of  $N_\theta = 400$  points separated by time steps  $\theta$ . The time

step  $\theta$  is set shorter than the relaxation time of the oscillator to keep the oscillator in the transient regime and generate temporal cascades at each sequence  $\tau$  of the pre-processed input.

We have developed a simple model based on a non-linear magnetic oscillator<sup>21</sup> taking into account the main ingredients for neuromorphic computing: non-linearity (square root dependence of the amplitude on the input current) and memory (relaxation time of the oscillator between two different output voltage levels). The dynamics of the evolution of the oscillator output microwave voltage  $V_i^{\text{osc}}$  as a function of the input voltage  $V_i^{\text{in}}$  at time step  $i$  can be solved numerically<sup>16</sup>:

$$V_i^{\text{osc}} = V_i^{\infty} \left( 1 - e^{-\Delta t / T_{\text{relax}}} \right) + V_{i-1}^{\text{osc}} \cdot e^{-\Delta t / T_{\text{relax}}}, \quad (2)$$

where  $T_{\text{relax}}$  is the relaxation time towards the asymptotic value  $V_i^{\infty}$  given by<sup>22</sup>:

$$V_i^{\infty} = c \sqrt{I_{\text{DC}} - V_i^{\text{in}} / R - I_{\text{c}}}, \quad (3)$$

with  $c$ , a constant related to the initial bias condition, i.e. the initial emitted voltage of oscillator,  $R$  the DC resistance of the oscillator and  $I_{\text{c}}$  the threshold current above which auto-oscillations can occur. In order to simulate the oscillator response to a time varying input ( $V_i^{\text{in}}$ ), we solve Eq. (2) numerically with the following parameters:  $\Delta t = 5$  ns,  $V_i^{\text{in}} / R = \pm 3$  mA,  $I_{\text{DC}} = 6$  mA,  $I_{\text{c}} = 4.9$  mA,  $T_{\text{relax}} = 410$  ns. These parameters are extracted from experiments as reported elsewhere<sup>8</sup>.

Even if the recognition rate by the non-linear filters (MFCC and cochleogram) is already high, there is still room for improvement with the inclusion of a recurrent neural network. The increase in the recognition rate induced by the emulated non-linear oscillator is shown in Fig. 4a. We determine the increase in recognition rate due to the neural network by subtracting from the total recognition rate the contribution from acoustic filters previously calculated in Fig. 2(a) and normalising the result with the total recognition rate. The gain provided by the non-linear oscillator is low for both non-linear filters: up to 4 % to 9.4 % (depending on the number of utterances used for training) for the cochlear method and 22 % for MFCC method. The increase is small because the total recognition rate (filter + network) is close to a perfect success rate: up to 99.8 % and 99.2 % for the cochleogram and the MFCC filter respectively. On the other hand, the neural network drastically improves the recognition gain up to 60.2 % (for 9 utterances trained) but the final recognition rate (filter + neural network) is not as good, around 70 %. The simulations have been obtained for a specific neural network based on the non-linear dynamics of an oscillator with time multiplexing in the framework of reservoir computing. As mentioned earlier, we choose this particular framework because it is frequently used for hardware implementations. However, these conclusions hold for very general types of (spatial or temporal) neural networks and learning processes because the limitation of the gain in recognition in the case of MFCC and cochlear filters is not due to the neural network but to the already excellent separation properties of the filtering.

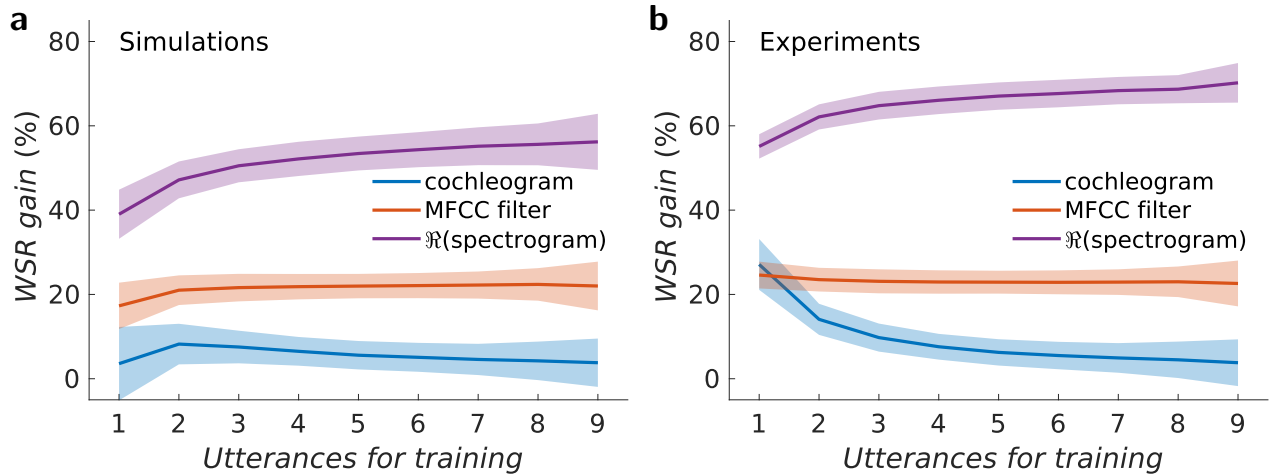


**Figure 4. Spoken digit recognition for a neural network.** (a) Spoken digit recognition rates as a function of the number of utterances  $N$  used during training for a non-linear oscillator modelled with Eqs.(2-3) and (b) experimental spin torque nano-oscillator driven by spin polarised current. The coloured region corresponds to the uncertainty of the recognition rate, here twice the standard deviation.

We compare these simulations to the behaviour of an experimental non-linear oscillator. In particular, we choose a magnetic nano-oscillator that was recently demonstrated to be an excellent building block for neuromorphic computing<sup>8, 16, 23</sup>. This kind of oscillator is small (nanoscale), performs low power computing, has a high signal to noise ratio for high reliable computation,

and allows a tunable non-linearity through the spin transfer torque mechanism. Our nanoscale oscillators are circular magnetic tunnel junctions, with a 6 nm thick FeB free layer and a diameter of 375 nm. The magnetisation in the FeB layer has a vortex structure as its ground state for these dimensions. In a small region called the vortex core, the elsewhere in-plane-curling magnetisation points out of the plane. Under dc current injection, the core of the vortex steadily gyrates around the centre of the dot with a frequency in the range 250 MHz to 400 MHz. Vortex dynamics driven by spin-torque are well-understood, well-controlled and have been shown to be particularly stable (more details can be found elsewhere<sup>24</sup>).

The experimental implementation of the spoken digit recognition task is described in Ref. <sup>8</sup>. The preprocessed input signal (filtered digits with time multiplexing) is generated and sent to the sample using an arbitrary waveform generator. Then, the microwave voltage across the magnetic tunnel junction is measured by a real time oscilloscope and fast oscillations are observed. The amplitude of oscillator response is obtained by inserting a microwave diode between the sample and the oscilloscope and is processed as the output signal. The oscillation amplitude is robust to noise thanks to the confinement provided by the counteracting torques exerted by the injected current and the magnetic damping. In addition, the voltage amplitude is highly non-linear as a function of the injected current. The current depends on the voltage amplitude similarly to our simulated oscillator (square root dependence) in Eq. (3). Furthermore, the amplitude of the oscillator voltage intrinsically depends on past inputs when the time step  $\theta$  is shorter than the relaxation time of the magnetic nano-oscillator. Therefore, this single nano-device has the two most crucial properties of neurons: non-linearity and memory.

The gain on the spoken digit recognition for the three different acoustic filters induced by the experimental magnetic nano-oscillator is shown in Fig. 4(b). There is very good agreement between the experimental results and the simulations. The gain varies between 4 % and 27 % for the cochleagram, 22 % and 24 % for the MFCC filter, and between 55 % and 70 % for linear spectrogram depending on the number of utterances used during the learning process. For some cases, the magnetic nano-oscillator exhibits slightly higher recognition gain than the simulations even though the latter neglects the intrinsic noise. We believe the better performance is mainly due to the higher complexity in the dynamics of the magnetic nano-oscillators, including a relaxation time that varies with current.

The different contributions to the spoken digit recognition task are summarised in Fig. 5 for the case in which nine utterances are used during the learning step and one during the recognition. The random choice level is 10 % and is shown in grey. The contribution of the filtering methods is shown in blue (not visible in the case of the linear spectrogram,  $\alpha = 1$ ). Fig. 5 also shows the net contribution of a neural network, in our case under the reservoir computing approach, to the spoken digit task. The simulated version of our neural network, i.e. using the simulated dynamics of the spin-torque vortex oscillators is shown in purple, while the results for the experimental magnetic nano-oscillators are shown in green. The main contribution to the spoken recognition task brought by the neural network happens when there is a lot of work to perform, i.e. when starting from the random choice level (linear spectrogram). Nevertheless, when our neural network is coupled with well performing stand-alone feature extraction techniques like the cochleagram or the MFCC filter, it is capable of bringing the recognition rate level to state-of-the-art values (99.8 % for MFCC filter + experimental spin-torque vortex oscillator).

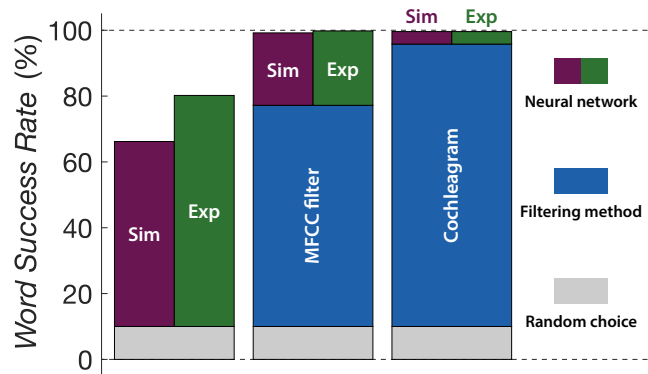


**Figure 5. Contributions to the spoken digit recognition rate.** Random choice level is shown in grey, the filtering methods in blue, and the neural network under the reservoir computing approach in purple and green for the simulations and experiments, respectively. Here we report for the situation where nine utterances are learned and one serves for the recognition test.

## Conclusion

We test different frequency filtering methods as stand alone feature extractors. Training a linear classifier on the  $R_\sigma$  vectors for the TI46 spoken digit data base, both the cochleagram and the MFCC filter give high identification rates without further

processing. On the other hand, the real part of a linear spectrogram does not separate the inputs of different digit classes. Non-linearly transforming the spectrogram, gives similar results to the cochleagram and MFCC filters, stressing that the separation found for the MFCC and cochlear classifiers is due to the presence of non-linearity, with a minor effect due to the particular type of non-linear transformation.

In a second part, a non-linear oscillator is added to process the filtered input. The gain in word recognition due to the non-linear oscillator is computed for each filtering method. The non-linear oscillator is simulated and found to be in excellent agreement with experimental results with magnetic nano-oscillators. For the non-linear methods MFCC and cochleagram, the gain of word recognition is small, despite a nearly perfect word recognition. On the other hand, for the linear spectrogram, the gain of word recognition is much higher even if the final word recognition is 70 % to 80 %.

An important lesson is that when evaluating hardware systems with speech recognition tasks, the final word recognition rate should be interpreted with caution. If a very efficient filtering is used to preprocess the input, the hardware system may not be adding much performance. A hardware system only adds something if it provides improved word recognition. In order to test and compare hardware systems, using a linear spectrogram eases the interpretation of the results, because it does not introduce any separation of the input prior the hardware system.

## References

1. LeCun, Y., Bengio, Y. & Hinton, G. Deep learning. *Nature* **521**, 436 (2015).
2. Mead, C. Neuromorphic electronic systems. *Proc. IEEE* **78**, 1629–1636, DOI: [10.1109/5.58356](https://doi.org/10.1109/5.58356) (1990).
3. Mead, C. & Ismail, M. (eds.) *Analog VLSI implementation of neural systems*, vol. 80 (Springer Science & Business Media, 2012).
4. Maass, W., Natschläger, T. & Markram, H. Real-time computing without stable states: A new framework for neural computation based on perturbations. *Neural Comput.* **14**, 2531–2560, DOI: [10.1162/089976602760407955](https://doi.org/10.1162/089976602760407955) (2002).
5. Jaeger, H. & Haas, H. Harnessing nonlinearity: Predicting chaotic systems and saving energy in wireless communication. *Science* **304**, 78–80, DOI: [10.1126/science.1091277](https://doi.org/10.1126/science.1091277) (2004).
6. Appeltant, L. *et al.* Information processing using a single dynamical node as complex system. *Nat. Commun.* **2**, 468 (2011).
7. Paquot, Y. *et al.* Optoelectronic reservoir computing. *Sci. Reports* **2**, 287 (2012).
8. Torrejon, J. *et al.* Neuromorphic computing with nanoscale spintronic oscillators. *Nature* **547**, 428 (2017).
9. Davis, S. & Mermelstein, P. Comparison of parametric representations for monosyllabic word recognition in continuously spoken sentences. *IEEE Transactions on Acoust. Speech, Signal Process.* **28**, 357–366, DOI: [10.1109/TASSP.1980.1163420](https://doi.org/10.1109/TASSP.1980.1163420) (1980).
10. Verstraeten, D., Schrauwen, B., Stroobandt, D. & Van Campenhout, J. Isolated word recognition with the liquid state machine: a case study. *Inf. Process. Lett.* **95**, 521 – 528, DOI: <https://doi.org/10.1016/j.ipl.2005.05.019> (2005). Applications of Spiking Neural Networks.
11. Hinton, G. *et al.* Deep neural networks for acoustic modeling in speech recognition. *IEEE Signal Process. Mag.* **29**, 82–97 (2012).
12. Lyon, R. A computational model of filtering, detection, and compression in the cochlea. In *ICASSP '82. IEEE International Conference on Acoustics, Speech, and Signal Processing*, vol. 7, 1282–1285, DOI: [10.1109/ICASSP.1982.1171644](https://doi.org/10.1109/ICASSP.1982.1171644) (1982).
13. Slaney, M. *Lyon's Cochlear Model*. Apple Computer, Inc., Cupertino, CA, apple computer technical report#13 edn. (1988).
14. Brunner, D., Soriano, M. C., Mirasso, C. R. & Fischer, I. Parallel photonic information processing at gigabyte per second data rates using transient states. *Nat. Commun.* **4**, 1364 (2013).
15. Vandoorne, K. *et al.* Experimental demonstration of reservoir computing on a silicon photonics chip. *Nat. Commun.* **5**, 3541 (2014).
16. Riou, M. *et al.* Neuromorphic computing through time-multiplexing with a spin-torque nano-oscillator. *Electron Devices Meet. (IEDM), 2017 IEEE Int.* 36.3.1–36.3.4, DOI: [10.1109/IEDM.2017.8268505](https://doi.org/10.1109/IEDM.2017.8268505) (2017).
17. Larger, L. *et al.* Photonic information processing beyond turing: an optoelectronic implementation of reservoir computing. *Opt. Express* **20**, 3241–3249, DOI: [10.1364/OE.20.003241](https://doi.org/10.1364/OE.20.003241) (2012).
18. Dejonckheere, A. *et al.* All-optical reservoir computer based on saturation of absorption. *Opt. Express* **22**, 10868–10881, DOI: [10.1364/OE.22.010868](https://doi.org/10.1364/OE.22.010868) (2014).

19. Vinckier, Q. *et al.* High-performance photonic reservoir computer based on a coherently driven passive cavity. *Optica* **2**, 438–446, DOI: [10.1364/OPTICA.2.000438](https://doi.org/10.1364/OPTICA.2.000438) (2015).
20. van der Maaten, L. & Hinton, G. Visualizing data using t-sne. *J. machine learning research* **9**, 2579–2605 (2008).
21. Slavin, A. N. & Tiberkevich, V. S. Nonlinear auto-oscillator theory of microwave generation by spin-polarized current. *IEEE Transactions on Magn.* **45**, 1875 –1918, DOI: [10.1109/TMAG.2008.2009935](https://doi.org/10.1109/TMAG.2008.2009935) (2009).
22. Grimaldi, E. *et al.* Response to noise of a vortex based spin transfer nano-oscillator. *Phys. Rev. B* **89**, 104404–, DOI: [10.1103/PhysRevB.89.104404](https://doi.org/10.1103/PhysRevB.89.104404) (2014).
23. Romera, M. *et al.* Vowel recognition with four coupled spin-torque nano-oscillators. *Nature* **563**, 230–234, DOI: [10.1038/s41586-018-0632-y](https://doi.org/10.1038/s41586-018-0632-y) (2018).
24. Tsunegi, S. *et al.* High emission power and q factor in spin torque vortex oscillator consisting of feb free layer. *Appl. Phys. Express* **7**, 063009 (2014).

## Acknowledgements

F.A.A. is a Research Fellow of the F.R.S.-FNRS. This work was supported by the European Research Council ERC under Grant bioSPINspired 682955.

## Author contributions statement

The study was designed by F.A.A, J.G., and M.D.S., samples were optimised and fabricated by S.T. and K.Y., experiments were performed by M.R. and J.T., and numerical studies were realised by F.A.A.. F.A.A. wrote the core of the manuscript and all authors contributed to the text as well as to the analysis of the results.

## Data Availability

The datasets generated during and/or analysed during the current study are available from the corresponding author on reasonable request.

## Additional information

The authors declare no competing interests.